UKRAINIAN JOURNAL OF MECHANICAL ENGINEERING AND MATERIALS SCIENCE

Vol. 9, No. 4, 2023

Iaroslav Lavrenko[1], Maksym Sushchenko[2], Oleksii Ishchenko[3]

[1] Department of Dynamics and Strength of Machine and Strength of Materials, National Technical University of Ukraine "Ihor Sikorsky Kyiv Polytechnic Institute", 37, Prospect Beresteiskyi (former Peremohy), Kyiv, Ukraine, e-mail: lavrenko.iaroslav@gmail.com.ua, ORCID 0000-0002-4384-4866

[2] Department of Dynamics and Strength of Machine and Strength of Materials, National Technical University of Ukraine "Igor Sikorsky Kyiv Polytechnic Institute", 37,Prospect Beresteiskyi (former Peremohy), Kyiv, Ukraine, e-mail: speadcubing@gmail.com, ORCID 0009-0007-5231-3817,

[3] Department of Dynamics and Strength of Machine and Strength of Materials, National Technical University of Ukraine "Ihor Sikorsky Kyiv Polytechnic Institute", 37, Prospect Beresteiskyi (former Peremohy), Kyiv, Ukraine, e-mail: i_94@ukr.net, ORCID 0000-0002-8314-9059

FREQUENCY RESPONSE AND STRENGTH ANALYSIS OF THE ELBOW ORTHOSIS PLANETARY GEARBOX SHAFT USING FEA

Received: August 22, 2023 / Revised: September 28, 2023 / Accepted: December 26, 2023

© *Lavrenko I., Sushchenko M., Ishchenko O., 2023*

https://doi.org/10.23939/ujmems2023.04.027

Abstract. Shafts of various sizes are used in various fields of mechanical engineering, automotive, marine and aerospace industries to transmit torque according to requirements. In this paper, we simulate and analyse the modal and harmonic response of a shaft on which a satellite of a planetary gearbox for an elbow orthosis is mounted. The orthoses are used during the rehabilitation of patients in the postoperative period or during the regeneration of lost limb functions. Steel 45 and PLA polylactide were used in the shaft modelling. The planetary gearbox shaft was analysed for modal and harmonic characteristics at three different torque values, i. e. 1732 N·mm, 3464 N·mm, 5196 N·mm, using ANSYS Workbench. The modal and harmonic analysis of the shaft stress-strain state is calculated, completed comparative analysis, and the vibration characteristics are discussed: shown natural frequencies, mode shapes, and harmonic response. Calculations for shaft durability under a complex stress state were performed, and safety factors were calculated for shafts made of steel 45 and PLA polylactide.

Key words: Gearbox; stress; deformation; vibration; frequency; fatigue; safety factor; ANSYS.

Introduction

Gearboxes are widely used in a variety of mechanical engineering applications. Depending on technical requirements and functions assigned to the mechanism, gearboxes can be different sizes, shapes and weights. In traumatology, there are strict requirements for mechanisms that can be used to rehabilitate patients. These include compactness, ease, reliability and safety for patients. One of these mechanisms is a planetary gearbox, which has a number of advantages, such as compactness and reliability, as the gearbox design consists of shafts and spur gears that have a high efficiency and gear ratios. Thus, the modernising task such a gearbox is to fulfil the conditions of ease and safety for patients.

Problem Statement

Mechanical shafts fail during operation for a variety reasons, but one of the main causes is destruction due to harmonic vibrations during operation. On the other hand, additive technologies, i.e. products made on a 3D printer, have been increasingly used in recent years. The advantage of such models is their cheapness, lightness and ease of manufacture, meaning that such parts can be created in difficult conditions, such as military operations. However, one of the disadvantages of this material is its rather

rapid destruction when materials are tired. Moreover, since these are polymeric materials, fracture can be both: plastic collapse and brittle. Thus, it is necessary to consider the safety of using polymeric materials in gearboxes under variable load.

This is a dynamic problem where natural frequencies of the mechanisms are controlled parameters, i.e. when designing gearbox parts, it must be ensured that it operates without resonance.

Review of Modern Information Sources on the Subject of the Paper

In recent years, scientists have made progress in studying dynamic processes in mechanical systems. The study results of the shaft stress-strain state (SSS) using the ANSYS software environment are presented by the authors in [1–3]. In article [4], the authors demonstrate the shaft modelling using the CATIA software environment, and results of static, dynamic analysis and fatigue calculations were taken by ANSYS software environment.

In order to identify hazards, the authors of [5] analysed static behaviour studies of a pump shaft model at design stage based on finite element method (FEM) under the influence of various types of load. In [6, 7], free pump shaft transverse vibrations with a complex geometry were investigated using analytical methods and numerical modelling. The modelling was created by taking into account stress concentrators. The results of shaft dimensions optimising and strength calculations using FEM are reported in [8, 9].

Study of rotor systems dynamic characteristics and defects influence on shaft characteristics are described by scientists in [10, 11, 12]. The authors of [13] calculated modal and harmonic analysis of a cylindrical gear without defects and with defects using ANSYS software environment. A comparative analysis of the results is presented.

To provide a reasonable explanation of the nature of vibration during planetary gearbox operation, research paper [14] presents a methodology for modelling its vibration signal. In [15], the authors propose method for modelling planetary gear residual stress field. Based on this modelling, a planetary gear finite-element model was constructed, dynamic meshing process was simulated, and effect of residual stresses was investigated.

The mechanical behaviour study of a spur gear for different materials, and fatigue life assessment, together with an understanding stresses behaviour at gear radii, is given by the authors in [16]. Therefore, dynamic characteristics study and high-speed elements stress-strain state determination of mechanical structures is an actual task.

In [17], the authors highlighted PLA polylactide mechanical characteristics, applications, and material advantages. In turn, the authors of [18] demonstrate research on determining ABS and PLA strength and elastic modulus as printed materials. The authors found that printed parts mechanical properties depend on printing parameters, and determined optimal printing parameters for required mechanical properties.

The authors in [19] demonstrate mechanical and geometric properties of 3-D printed composite parts carbon fibres. Tensile, bending, and interlayer shear strength tests were conducted by the authors to obtain the tested samples mechanical characteristics.

Objectives and problems of research

In developing a reliable structure, it is necessary to more accurately determine its SSS and study its dynamic characteristics. Since full-scale tests are quite expensive, using numerical modelling software products is an urgent task.

This paper purpose is study real shaft structure of planetary gearbox dynamic characteristics for an elbow orthosis to determine shaft natural frequencies, modes, and safety factor made of steel and PLA.

Since shafts operate at high rotational speeds during operation, the natural frequencies calculations and their analysis is important to determine resonant frequencies that lead decrease in functionality.

Main material presentation

The design scheme of the gearbox satellite shaft with its main dimensions is shown in Fig. 1, *a*. During its operation, a moment in an opposite clockwise direction is mounted, occurs on the shaft on

which the gearbox satellite. Creating the shaft geometry according to the design scheme is first step of the analysis (Fig. 1, *b*). For this purpose, we used a CAD system such as SOLIDWORKS.

The next step is to create an adequate finite element model based on the created geometric model in the ANSYS Workbench software environment and validate this model. The easiest way is to check model natural vibration frequencies with taking into account the initial stresses and boundary conditions, is analytically and by FEM for steel 45, since its mechanical characteristics are well known. In this case, a sufficient number of FEM elements and nodes is determined. The choice of meshing method and element size depends on structure geometry. In this study, a hexahedral finite element is used, as it is the most simpliest shape for which the subsequent interpolation has the smallest error.

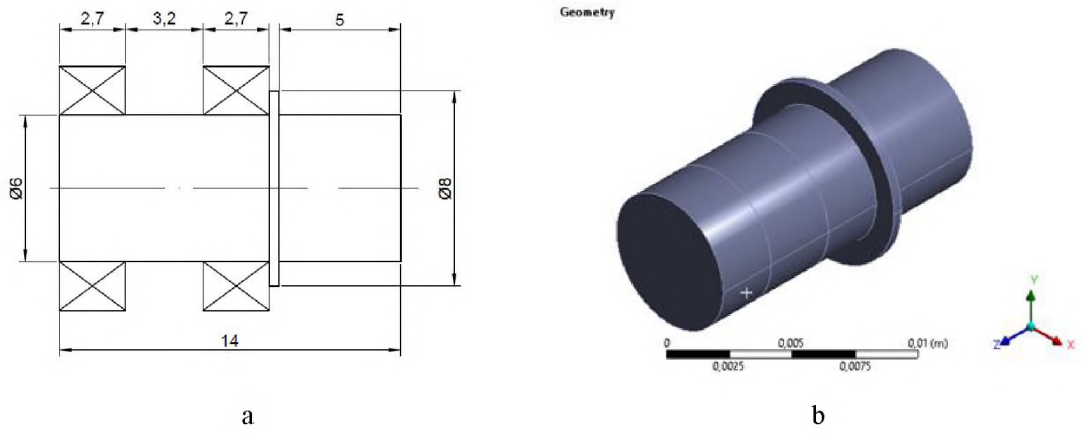

a b

Fig. 1. Sketch (a) and geometry model (b) of the planetary gearbox satellite shaft

The next step of the study is modal and harmonic analysis. The modal analysis obtained the shaft natural frequencies and vibration modes, and the harmonic analysis obtained the deformation and stress amplitudes for each natural frequency of the structures under excitation loads.

As one of the study objectives is the safety for using polymers in structures that can be printed on a 3D printer, such a shaft will be evaluated using most commonly used 3D plastic, PLA, at different printing angles. When evaluating the shaft for fatigue with polymers (PLA and PLA45), the characteristics obtained from the experimental data [17–19] will be used, since their fatigue behaviour is still being studied and is quite scattered.

In creation of a finite element model, the most common method is to control results convergence while ensuring a sufficient elements number. In other words, when comparing meshes with different element densities, it is necessary to select one that, when densified, will hardly change the result. Initially, we selected automatically built meshes in the ANSYS Workbench software environment with element sizes of 5 mm, 0.5 mm, 0.3 mm.

For a comparative analysis of meshes of different densities, shaft analytical model fixed support at one end and with a concentrated mass at the other end was created [20].

The material characteristics used in the calculation for steel 45 are given in Table 1.

Table 1

Material properties steel 45

Parameter	Units of measure	Value
Density	kg/m^3	7850
Thermal expansion coefficient	C^{-1}	$1.2 \cdot 10^{-5}$
Young modulus	Pa	$2 \cdot 10^{11}$
Poisson's ratio		0.3
Shear modulus	Pa	$7.69 \cdot 10^{10}$

The results of the comparative mesh and analytical calculations are presented in Table 2.

Table 2

Results of the mesh comparison

Element size, mm	Frequency (Ansys), Hz	Calculation time, sec	Frequency (analytically), Hz	Accuracy, %
5	104300	4	94622	10.23
0.5	100420	136	94622	6.13
0.3	100390	1866	94622	6.1

As can be seen from the data in Table 2, the mesh with a maximum finite element size (5 mm) has a significant accuracy compared to the analytical calculation. The highest accuracy is obtained with a mesh with a finite element size of 0.3 mm, but the calculation time is much longer than for a mesh with a 0.5 mm element, and the calculation accuracy is almost the same. Therefore, there is no point in further reducing the mesh size. All further calculations will be using finite elements with a size of 0.5 mm and an average element surface area of 0.262 mm². Thus, the shaft has 8325 finite elements and the total number of nodes is 30409 (Fig. 2).

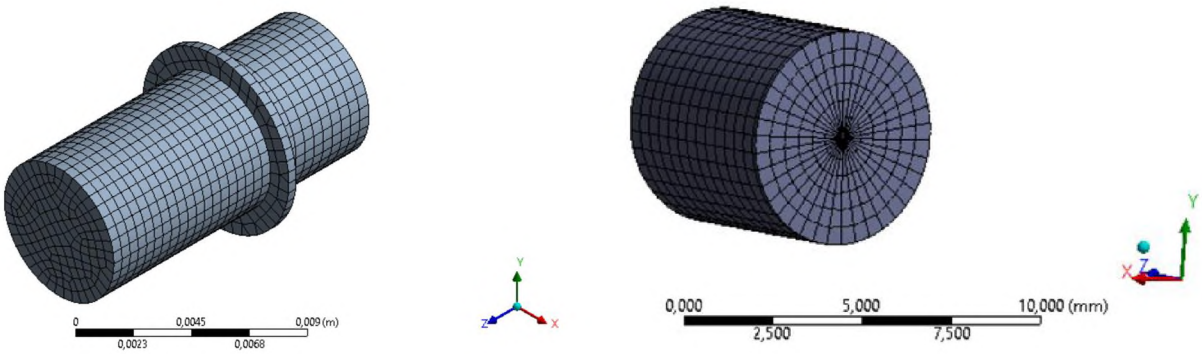

Fig. 2. Selected FEM

A similar comparative calculation was performed for another material, polylactide PLA. The mechanical characteristics for PLA are shown in Table 3.

Table 3

Material properties PLA

Parameter	Units of measure	Value
Density	kg/m^3	1250
Thermal expansion coefficient	C^{-1}	$1.2 \cdot 10^{-5}$
Young modulus	Pa	$3.27 \cdot 10^9$
Poisson's ratio		0.3
Shear modulus	Pa	$2.73 \cdot 10^9$

The first bending frequency for a shaft made of plastic was determined analytically and using ANSYS. A comparative analysis is given in Table 4.

From the data in Table 4, an error of 5.18 % was determined, i.e., when reducing the system mass, due to the polymer lower density compared to steel, the bump mass plays a role, which is not taken into account in the analytical model.

Table 4

Results of calculating the first natural frequency

Element size, mm	Frequency (Ansys), Hz	Frequency (analytically), Hz	Calculation time, sec	Accuracy, %
0.5	32124	30459	136	5.18

Boundary conditions play an important role in finite element analysis. The shaft is supported by fixed bearings. The planetary gearbox satellite shaft of the elbow orthosis fixation is shown in Fig. 3. The moment that occurs on the shaft during planetary gearbox of the elbow orthosis operation is converted into an equivalent force and applied to the shaft, as shown in Fig. 4.

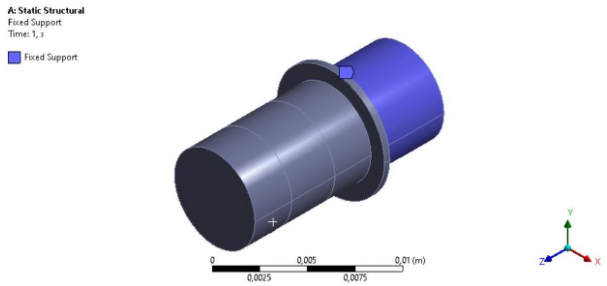

Fig. 3. Fixed support of the shaft

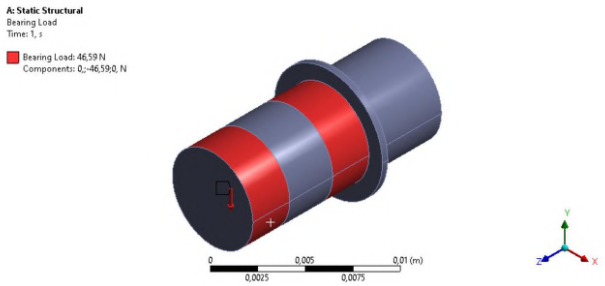

Fig. 4. Bearing load applied to the shaft

The modal analysis method is taking modes, find natural frequencies and can be solved using appropriate FEM software. Harmonic analysis is performed to find the deformation and stress amplitudes for each found natural frequency of the structures under the excitation loads. The gearbox shaft was designed using SOLIDWORKS and analysed using ANSYS Workbench.

Modal response of the steel shaft. Modal analysis is performed to obtain the vibration characteristics for the planetary gearbox satellite shaft, such as natural frequencies and vibration modes.

The calculation was limited to the tenth waveform (247840 Hz) with a modal deformation (0.26246 mm) (Table 5). The minimum frequency was obtained for the first vibration mode (100410 Hz) with the corresponding modal displacement (0.038727 mm) in bending.

Table 5

Eigenfrequencies and corresponding maximum displacement for steel 45 shaft

No.	Frequency, Hz	Modal deformation, mm	Type of deformation
1	100410	0.038727	Bending form (1 wave)
2	100410	0.038728	Duplicate bending form (1 wave)
3	110990	0.036701	Torsional form (1 wave)
4	177580	0.026249	Longitudinal form
5	198890	0.042367	Bending form (2 wave)
6	198900	0.042374	Bending form (2 wave)
7	216160	0.040369	Torsional form (2 wave)
8	243070	0.3059	Not applicable to the main shaft
9	243600	0.28998	Not applicable to the main shaft
10	247840	0.26246	Not applicable to the main shaft

The first 10 shaft vibration modes and their corresponding natural frequencies are shown in Fig. 5.

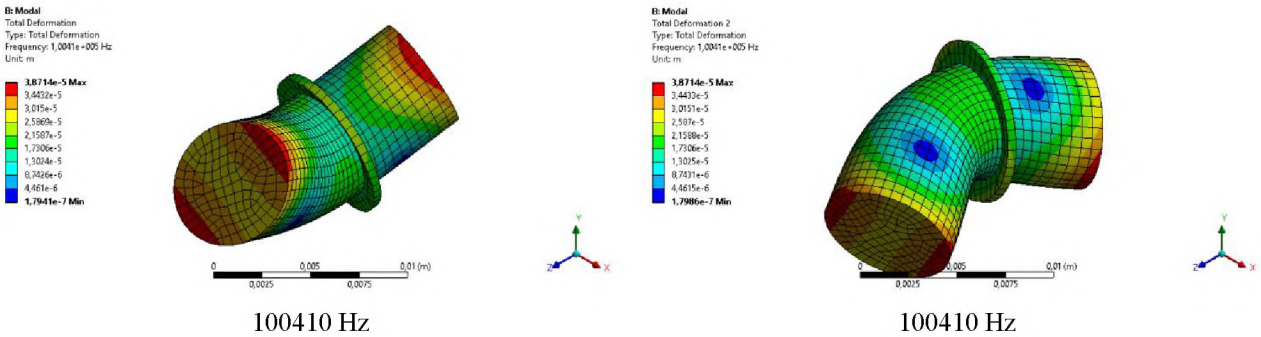

100410 Hz

100410 Hz

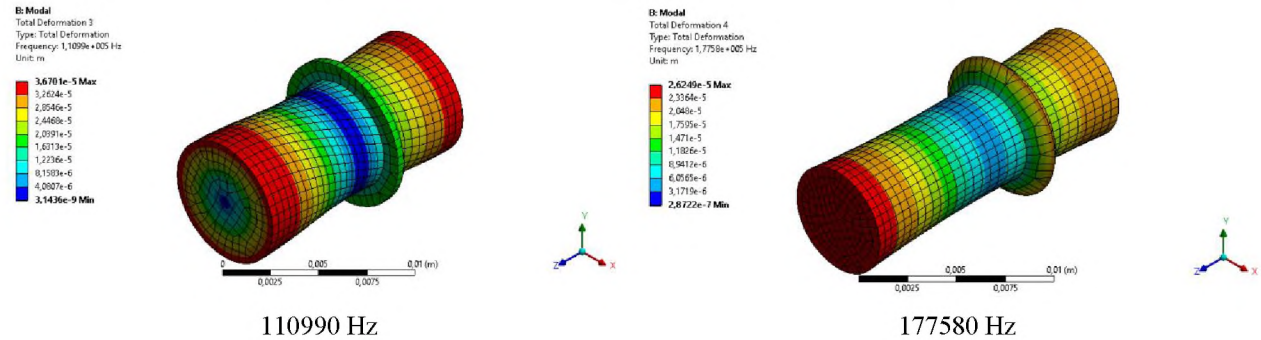

110990 Hz

177580 Hz

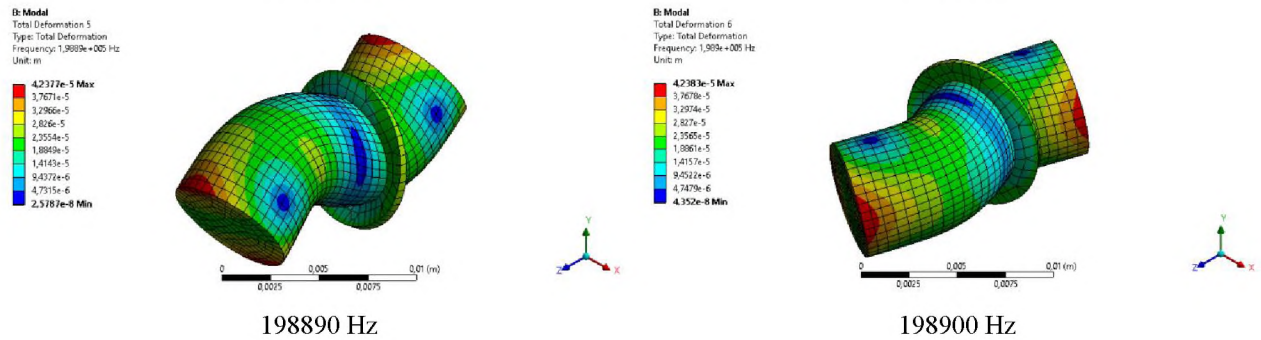

198890 Hz

198900 Hz

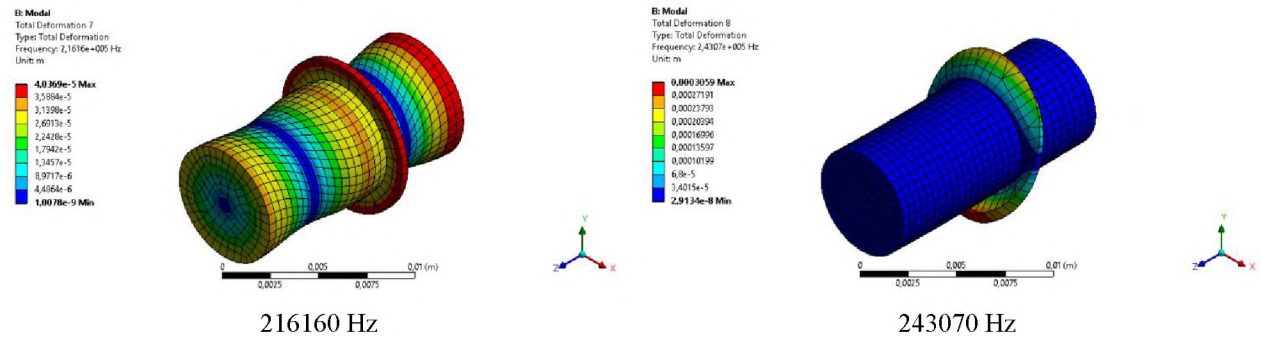

216160 Hz

243070 Hz

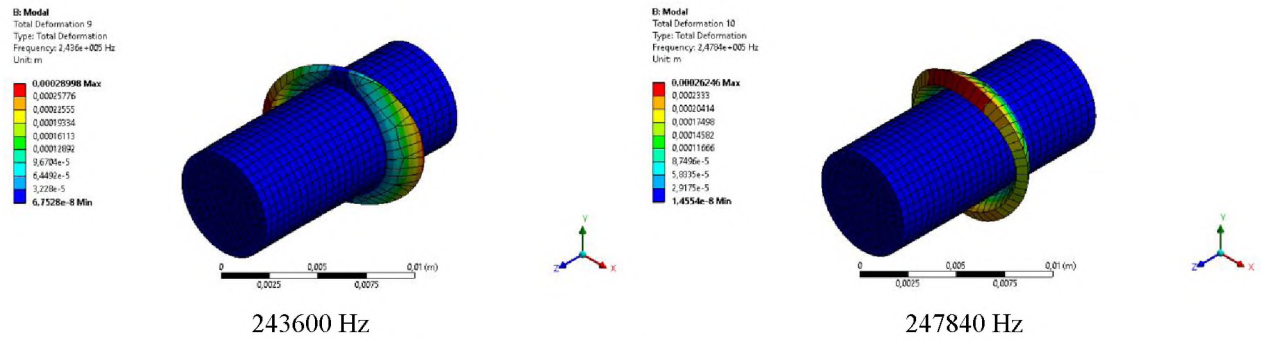

243600 Hz

247840 Hz

Fig. 5. Total deformation of the shaft from Mode 1–10 using ANSYS

Modal response of the PLA, PLA 45 shaft. Similar calculations to determine the natural frequencies and vibration forms were for a planetary gearbox shaft made of plastic: PLA and PLA 45. The results of the simulation are shown in Table 6.

Table 6

Eigenfrequencies and corresponding maximum displacement for PLA shaft

No.	Frequency, Hz	Modal deformation, mm	Type of deformation
1	32177	0.097016	Bending form (1 wave)
2	32178	0.097018	Duplicate bending form (1 wave)
3	35566	0.091973	Torsional form (1 wave)
4	56907	0.06578	Longitudinal form
5	63735	0.1062	Bending form (2 wave)
6	63737	0.10621	Bending form (2 wave)
7	69268	0.10116	Torsional form (2 wave)
8	77892	0.76658	Not applicable to the main shaft
9	78062	0.72668	Not applicable to the main shaft
10	79420	0.65772	Not applicable to the main shaft

The natural vibration modes obtained as a result of the modal analysis are shown in Fig. 6, and the corresponding natural frequencies are also given.

The natural frequencies results for Steel 45 and PLA, PLA 45 (Fig. 7) and modal deformation for Steel 45 and PLA, PLA 45 (Fig. 8) during the simulation are presented in the form of histograms depending on their modal modes, respectively.

Harmonic response of the steel 45 shaft. The harmonic analysis for the planetary gearbox satellite shaft of the elbow orthosis made with steel 45 is calculated when torques of 1732 N·mm, 3464 N·mm, 5196 N·mm (100 %, 200 %, 300 %) are applied. The resulting graphical distribution of deformation for a frequency 250 kHz along the shaft structure, taking into account the corresponding torques, is shown in Fig. 9, Fig. 12, and Fig. 15. Harmonic analysis is necessary to determine the frequency and phase response of the satellite shaft in operating frequency range, which is solved by modal analysis and for the current study, the operating frequency range varies from 0 to 250,000 Hz. In the plot of amplitude (mm) versus frequency (Hz), it is found that a deformation decrease in the frequency range from 50,000 Hz and a sudden increase is observed in the frequency range of 10.000 Hz and 11.500 Hz, followed by a deformation drop and a gradual decrease. The maximum deformation (0.000016 mm) is taken in the X-direction and the minimum deformation is taken in the Z-direction (Fig. 10).

Then, the graph of stress amplitude (Pa) versus frequency (Hz) shows that the maximum stress (10544 Pa) is taken in the X direction (Fig. 11). The identical dependence of deformation amplitude (mm) and stress (Pa) on frequency (Hz) is taken in the planetary gearbox shaft of the elbow orthosis harmonic analysis simulation at torque of 3464 N·mm (Fig. 13, Fig. 14) and 5196 N·mm (Fig. 16, Fig. 17) due to their linear loads, respectively.

The presented deformation amplitude graphs and normal stresses make it possible to determine the maximum values in each direction.

Harmonic response of the PLA, PLA 45 shaft. The harmonic analysis for the planetary gearbox satellite shaft of the elbow orthosis made with PLA polylactide is calculated as for the steel shaft. The calculation results are shown in Fig. 18–20 for an applied torque 1732 N·mm, in Fig. 21–23 for a torque 3464 N·mm, and in Fig. 24–26 for a torque 5196 N·mm. The figures show that the maximum displacement amplitudes are up to 0.016 mm, and the maximum stresses are up to 40 kPa along the Z-axis. Since the obtained deformation and stresses results are insignificant, it is advisable to make further calculations for fatigue strength.

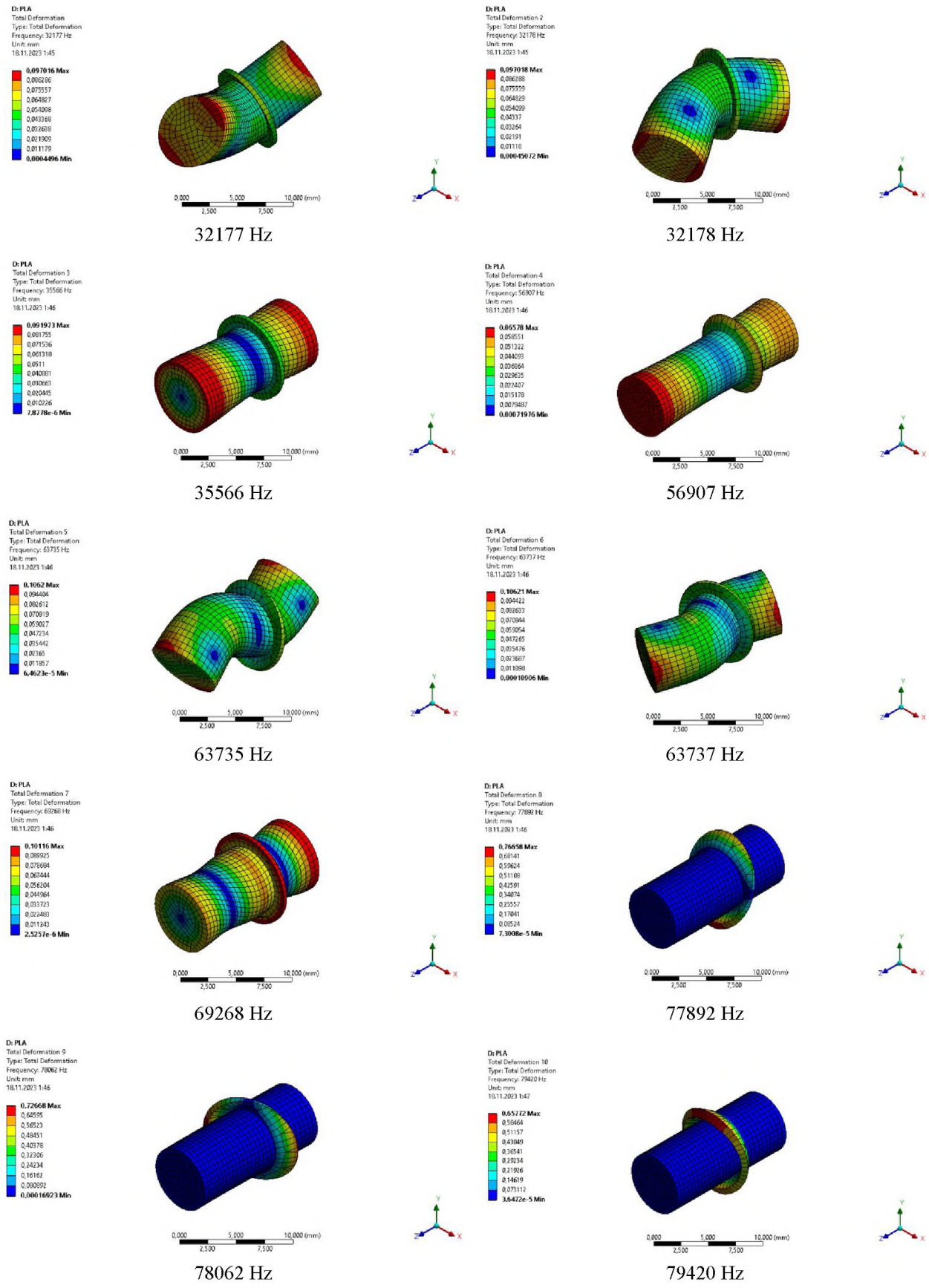

Fig. 6. Total deformation of the shaft from Mode 1–10 using ANSYS

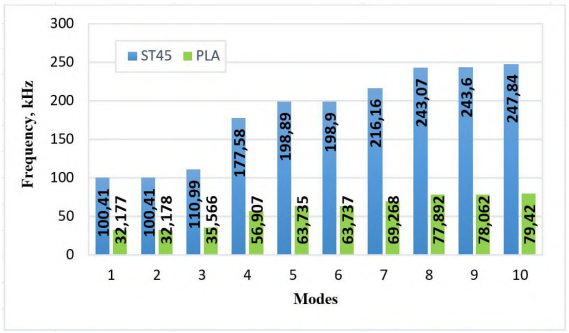

Fig. 7. Frequency (kHz) v/s Modes

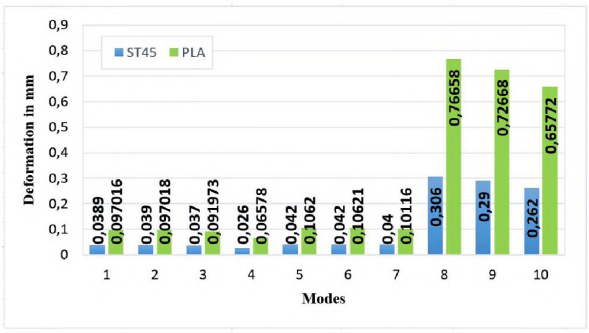

Fig. 8. Deformation (mm) v/s Modes

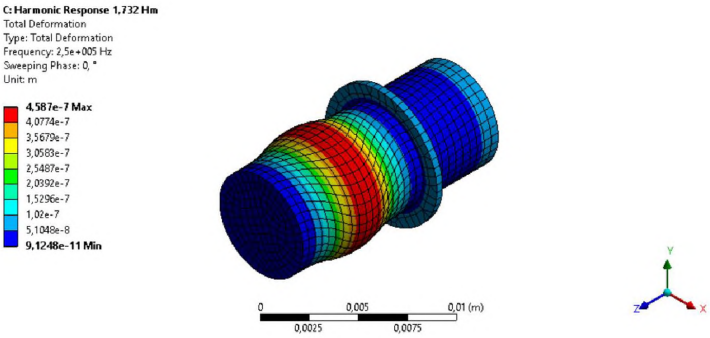

Fig. 9. Total deformation at 1732 N·mm

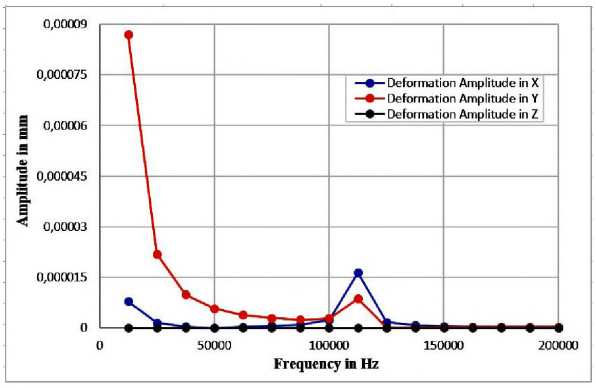

Fig. 10. Deformation Amplitude (mm) v/s Frequency (Hz) at 1732 N·mm

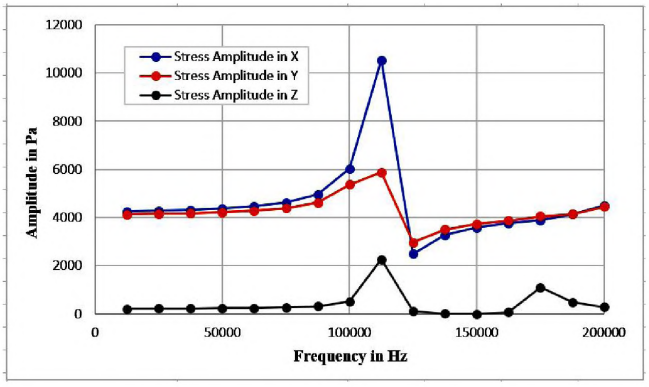

Fig. 11. Stress Amplitude (Pa) v/s Frequency (Hz) at 1732 N·mm

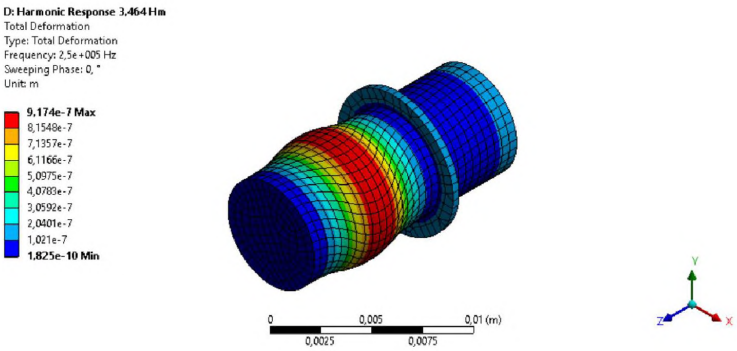

Fig. 12. Total deformation at 3464 N·mm

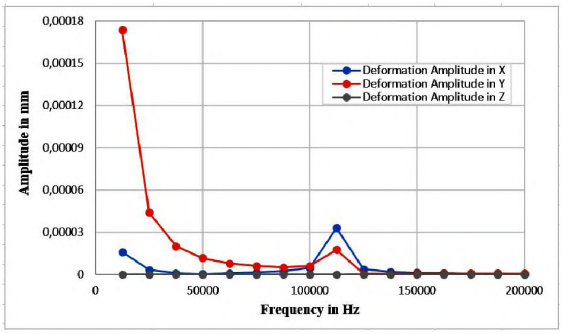

Fig. 13. Deformation Amplitude (mm) v/s Frequency (Hz) at 3464 N·mm

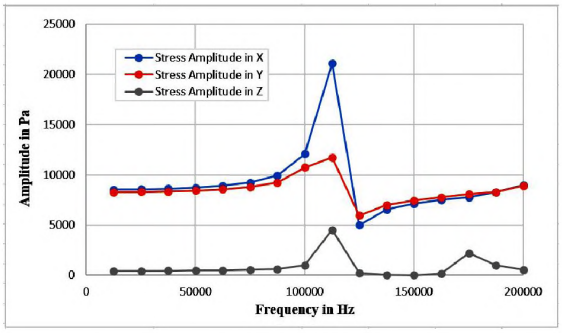

Fig. 14. Stress Amplitude (Pa) v/s Frequency (Hz) at 3464 N·mm

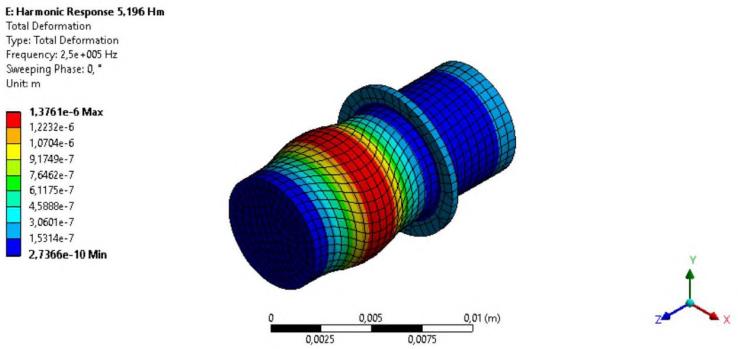

Fig. 15. Total deformation at 5196 N·mm

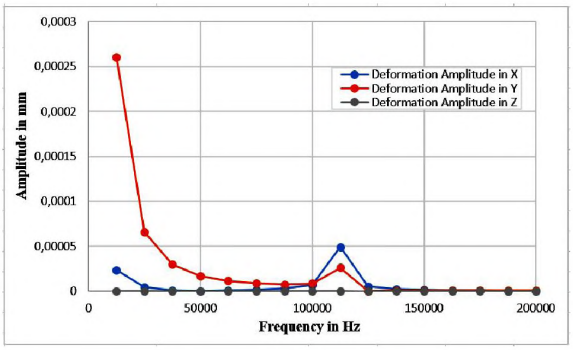

Fig. 16. Deformation Amplitude (mm) v/s Frequency (Hz) at 5196 N·mm

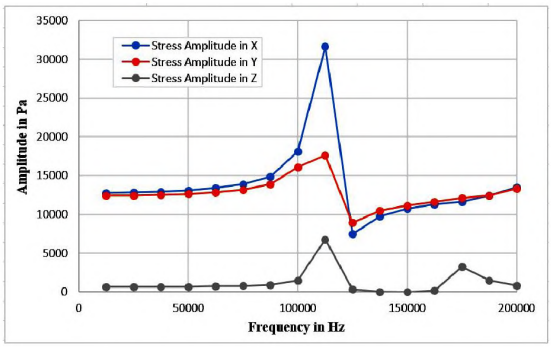

Fig. 17. Stress Amplitude (Pa) v/s Frequency (Hz) at 5196 N·mm

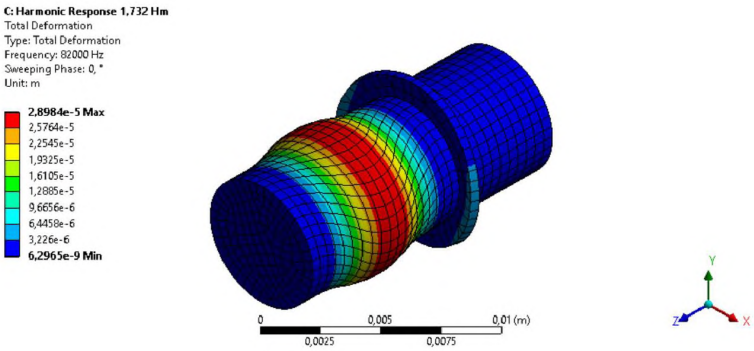

Fig. 18. Total deformation at 1732 N·mm

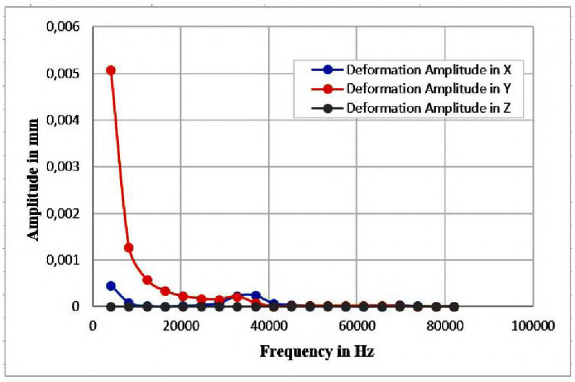

Fig. 19. Deformation Amplitude (mm) v/s Frequency (Hz) at 1732 N·mm

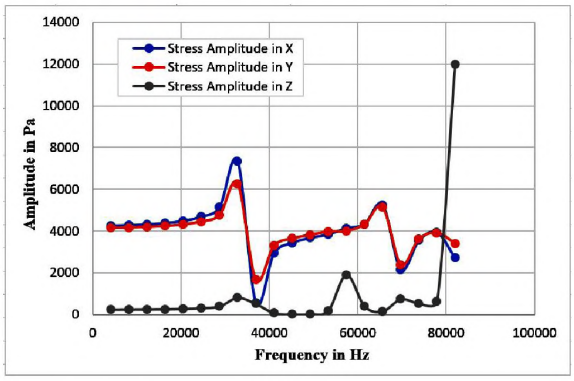

Fig. 20. Stress Amplitude (Pa) v/s Frequency (Hz) at 1732 N·mm

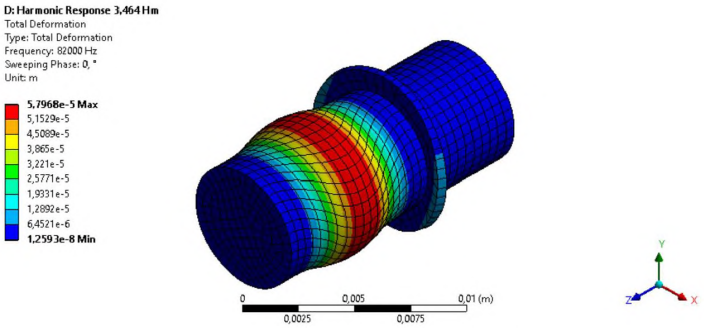

Fig. 21. Total deformation at 3464 N·mm

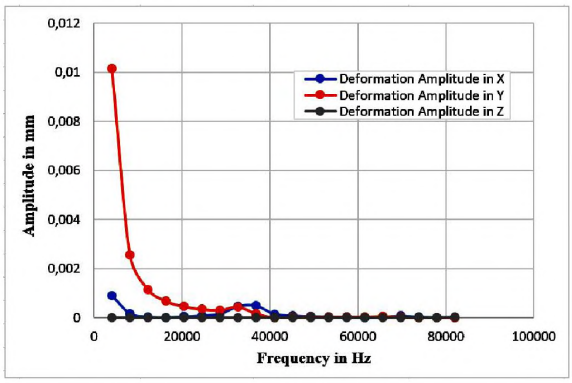

Fig. 22. Deformation Amplitude (mm) v/s Frequency (Hz) at 3464 N·mm

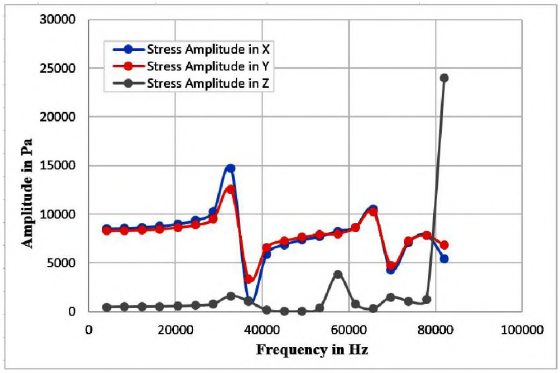

Fig. 23. Stress Amplitude (Pa) v/s Frequency (Hz) at 3464 N·mm

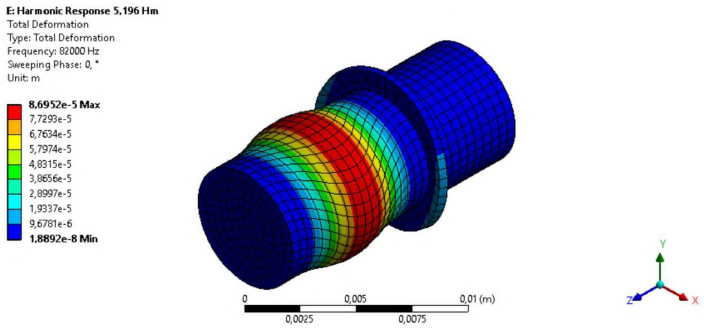

Fig. 24. Total deformation at 5196 N·mm

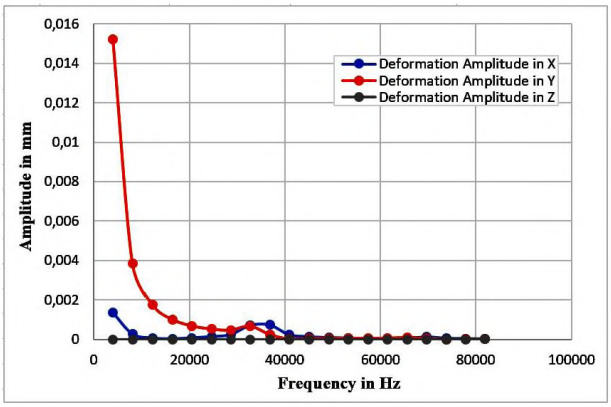

Fig. 25. Deformation Amplitude (mm) v/s Frequency (Hz) at 5196 N·mm

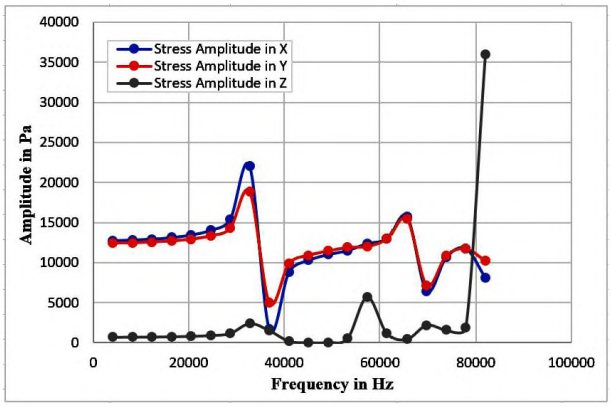

Fig. 26. Stress Amplitude (Pa) v/s Frequency (Hz) at 5196 N·mm

Fatigue calculation under a complex stress state for a steel shaft. An analytical and numerical fatigue calculation was performed to determine the safety factor and compare it with the permissible value.

The analytical calculation was performed according to [21]. To determine the safety factor, it is necessary to take the stresses in the dangerous shaft sections where his diameter change. The bending moment in the dangerous section is 0.2 N·m, the torque is 1.732 N·m, the axial moment of resistance is $W_1 = 0.1 \cdot 0.006^3 = 2.16 \cdot 10^{-8}\ m$, while the polar moment of resistance is $W_2 = 0.2 \cdot 0.006^3 = 4.32 \cdot 10^{-8}\ m$.

Normal and shear stresses in the dangerous section are calculated according to Eq. (1) and Eq. (2), respectively.

$$\sigma_a = \frac{M}{W_1} = \frac{0.2}{2.16 \cdot 10^{-8}} = 9.27\ MPa, \tag{1}$$

$$\tau_a = \frac{M_k}{2 \cdot W_2} = \frac{1.732}{2 \cdot 4.32 \cdot 10^{-8}} = 20.05\ MPa. \tag{2}$$

The concentration factors for normal and shear stresses in a dangerous section [18] are determined according to Eq. (3) and Eq. (4), respectively.

$$(K_\sigma)_D = \left(\frac{K_\sigma}{K_d} + K_f - 1\right) \cdot \frac{1}{K_y} = \left(\frac{2.1}{0.7} + 1 - 1\right) \cdot \frac{1}{2} = 1.5, \tag{3}$$

$$(K_\tau)_D = \left(\frac{K_\tau}{K_d} + K_f - 1\right) \cdot \frac{1}{K_y} = \left(\frac{1.43}{0.7} + 1 - 1\right) \cdot \frac{1}{2} = 1.02, \tag{4}$$

where K_σ, K_τ – effective stress concentration factors; K_d – influence factor of the absolute cross-sectional size; K_f – roughness influence factor; K_y – coefficient of surface hardening influence.

The fatigue limits in the dangerous section are calculated according to Eq. (5) and Eq. (6):

$$(\sigma_{-1})_D = \frac{\sigma_{-1}}{(K_\sigma)_D} = \frac{245}{1.5} = 163.33\ MPa, \tag{5}$$

$$(\tau_{-1})_D = \frac{\tau_{-1}}{(K_\varsigma)_D} = \frac{142.1}{1.02} = 139.31\ MPa, \tag{6}$$

where is the fatigue limit of a smooth specimen made of steel 45 $\sigma_{-1} = 245\ MPa$, $\tau_{-1} = 0.58 \cdot 245 = 142.1\ MPa$.

The safety factors determined by normal and shear stresses are calculated according to Eq. (7) and Eq. (8).

$$S_\sigma = \frac{(\sigma_{-1})_D}{\sigma_a} = \frac{163.33}{9.27} = 17.62, \tag{7}$$

$$S_\tau = \frac{(\tau_{-1})_D}{\tau_a} = \frac{139.31}{20.05} = 6.94. \tag{8}$$

The total safety factor was obtained using the Gough-Pollard formula according to Eq. (9).

$$S = \frac{S_\sigma \cdot S_\tau}{\sqrt{S_\sigma^2 + S_\tau^2}} = \frac{17.62 \cdot 6.94}{\sqrt{17.62^2 + 6.94^2}} = 6.46. \tag{9}$$

To validate the safety factor calculation, a numerical fatigue calculation was performed using the ANSYS software environment. The calculation results are shown in Fig. 27.

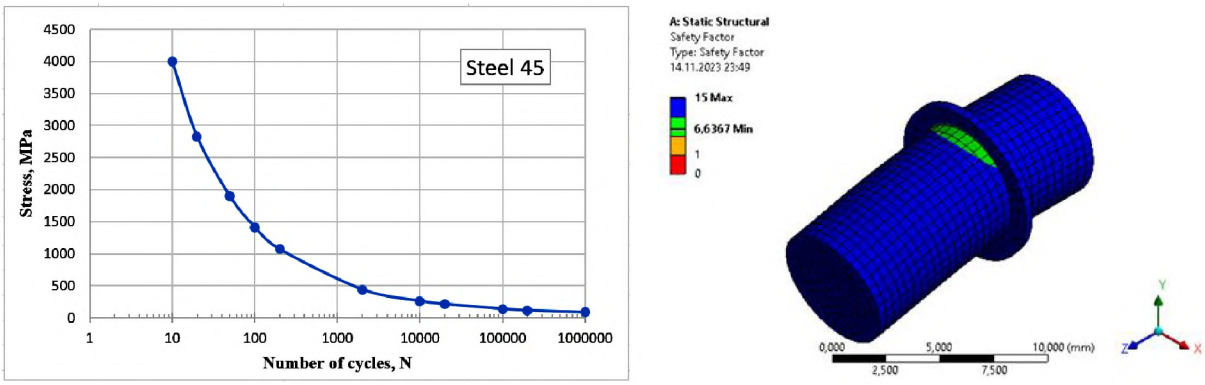

a b

Fig. 27. Fatigue curve (a) for steel 45 and safety factor (b) (ANSYS)

The results of the comparative analysis of determining the safety factor are shown in Table 7.

Table 7

Results of calculation of the safety factor

Ansys	Analytically	Accuracy, %
6.6367	6.4572	2.71

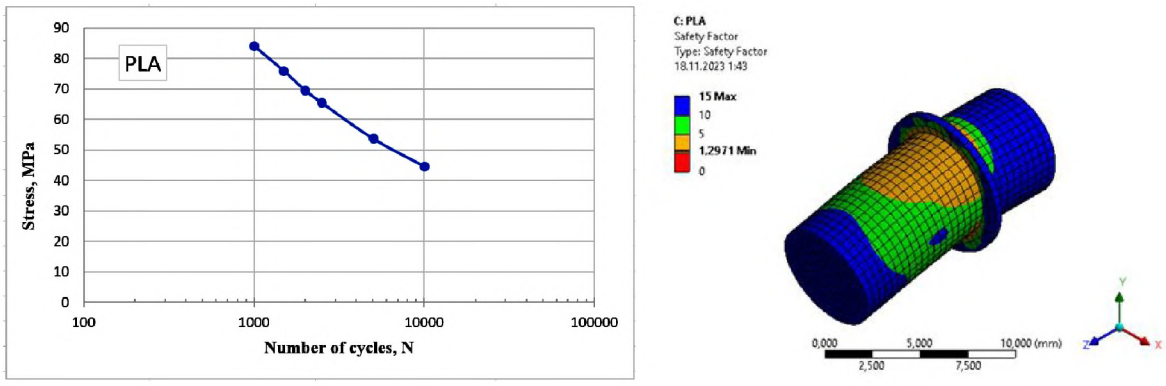

a b

Fig. 28. Fatigue curve (a) for PLA and safety factor (b) (ANSYS)

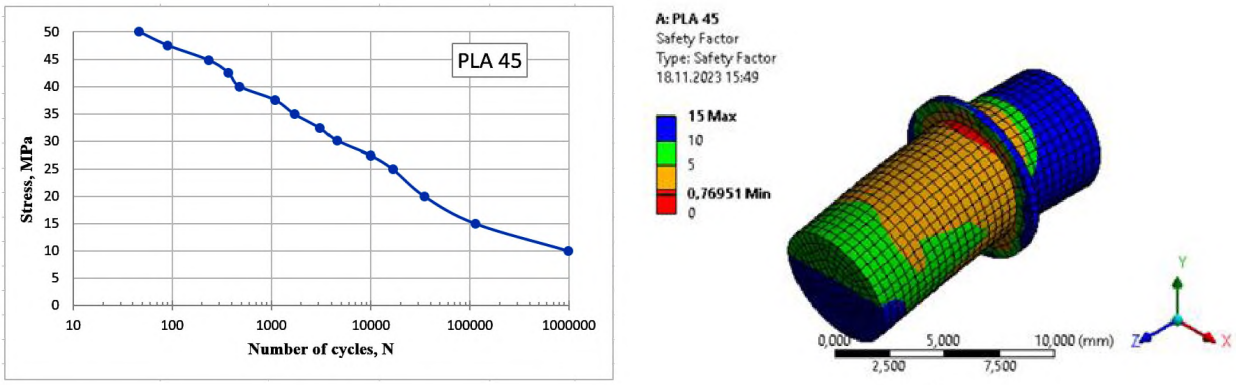

a b

Fig. 29. Fatigue curve (a) for PLA 45 and safety factor (b) (ANSYS)

Fatigue calculation under complex stress state for PLA, PLA 45 shaft. A numerical fatigue calculation was performed to determine the safety factor. It was calculated using the ANSYS software environment and experimental values of PLA plastic for different printing angles (Fig. 28, *a* and Fig. 29, *a*) [22]. The calculation results are shown in Fig. 28, *b* and Fig. 29, *b*, respectively.

It can be seen from the figures that the safety factor is provided for the material in which printing was provided orthogonal to the load. The transition from the shoulder to the main body of the shaft is a dangerous area.

Conclusions

Based on the results obtained, the following conclusions were made as a result of the modal and harmonic analysis for the planetary gearbox satellite shaft of the elbow orthosis using the ANSYS Workbench software environment.

From the modelling results, we can see that the first 6 natural frequencies are equal to or close to 0 Hz. This can be explained by the fact that a solid body has six degrees of freedom, three displacements and three rotations. In a static structural model, we need to constrain all six degrees of freedom because ANSYS cannot solve the problem. If one of the DOFs has no constraints, it means that the stiffness in that direction is zero. If a solid has no constraints, there are six zero frequency modes. The next 10 frequencies given in the paper have large values – more than 100 kHz. This is due to the small size and weight of the shaft body (about one centimetre).

The analysis of the harmonic characteristics is shown in the corresponding figures. During the simulation, the torque was increased. The calculation showed small values of stresses and deformation for both the steel and polymer shafts, which indicates the correct shaft shape and size.

A further calculation planetary gear shaft of the elbow orthosis for fatigue was performed. It was found that the safety factors for the 45 steel shaft obtained by analytical and numerical methods have great convergence and the strength is provided. The safety factors for polylactide PLA, PLA 45, are approximately 1.3 and 0.8, respectively. In this case, there is a need for further selection of the polymeric material and determination their fatigue characteristics at different printing angles with a 3-D printer to provide recommendations for checking such parts after their manufacture.

References

[1] N. Lenin Rakesh, et al., "Stress analysis of a shaft using Ansys", *Middle-east Journal of Scientific Research*, 12 (12), ISSN 1990-9233, pp. 1726–1728, 2012.

[2] P. Krishna Teja, et al., "Finite element analysis of propeller shaft for automotive and naval application", *International Research Journal of automotive Technology*, Vol. 1, Issue 1, ISSN 2581-5865, pp. 8–12, 2018.

[3] S. D. Dere, and L. Dhamande, "Rotor bearing system FEA analysis for misalignment", *International journal of advance research and innovative ideas in education*, Vol. 3, Issue 4, pp. 2102–2112, 2017.

[4] B. Gaikwad Rushikesh, and V. Gaur Abhay, "Static and dynamic analysis of shaft (EN24) of foot mounting motor using FEA", *International Journal of Innovations in Engineering Research and Technology,* Vol. 5, Issue 6, ISSN: 2394-3696, pp. 57–70, 2018.

[5] A. Asonja, et al., "Analysis of the static behavior of the shaft based on finite method under effect of different variants of load", *Applied Engineering Letters*, Vol. 1, No. 1, pp. 8–15, ISSN: 2466-4847, 2016.

[6] S. Noga, et al., "Analytical and numerical analysis of injection pump (Stepped) shaft vibrations using Timoshenko theory", *Acta mechanica et automatica,* Vol. 16, no. 3, pp. 215–224, 2022.

[7] P. B. Sob, "Modelling and simulating stress distribution on a centrifugal pump shaft during backpressure", *International Journal of Engineering Research and Technology*, Vol. 13, No. 10, ISSN 0974-3154, pp. 2943–2954, 2020.

[8] J. Joshi, et al., "Design analysis of shafts using simulation softwares", *International Journal of Scientific and Engineering Research*, Vol. 5, Issue 8, ISSN 2229-5518, pp. 751–761, 2014.

[9] N. Rasovic, et al., "Design and analysis of steel reel shaft by using FEA", *Tehnicki vjesnik*, Vol. 26, Issue 2, pp. 527–532, 2019.

[10] S. M. Ghoneam, et al., "Dynamic analysis of rotor system with active magnetic bearings using finite element method", *International Journal of Engineering Applied Sciences and Technology,* Vol. 7, Issue 1, ISSN 2455-2143, pp. 09–16, 2022.

[11] B. Thomas, et al., "Dynamic analysis of functionally graded shaft", *FME Transactions,* Vol. 47, Issue 1, pp. 151–157, 2019.

[12] M. J. Jweeg, et al., "Dynamic analysis of a rotating stepped shaft with and without defects", *IOP Conf. Series: Materials Science and Engineering, 3rd International Conference on Engineering Sciences,* Kerbala, Iraq, Vol. 671, 2020.

[13] R. Kurbet, V. Doddaswamy, C.M. Amruth, Mohammed Rafi H. Kerur, S. Ghanaraja, "Frequency response analysis of spur gear pair using FEA", *Materials Today: Proceedings,* 52 (2022), pp. 2327–2338.

[14] X. Liang, M. J. Zuo and W. Chen, "Dynamics-Based Vibration Signal Modeling for Tooth Fault Diagnosis of Planetary Gearboxes", *Fault diagmosis and Detection*, 2017. http://dx.doi.org/10.5772/67529

[15] J. Wang, Y. Wang and Z. Huo. Finite Element Residual Stress Analysis of Planetary Gear Tooth. *Hindawi Publishing Corporation Advances in Mechanical Engineering*, Vol. 2013, Article ID 761957, 12 p. http://dx.doi.org/10.1155/2013/761957

[16] P. Silori, A. Shaikh, N. Kumar K. C., T. Tandon, "Finite Element Analysis of Traction gear using ANSYS", *Materials Today: Proceedings,* 2, pp. 2236–2245, 2015.

[17] S. Farah, D. G. Anderson, R. Langer, "Physical and mechanical properties of PLA, and their functions in widespread applications — A comprehensive review", *Advanced Drug Delivery Reviews*, vol. 107, pp. 367–92, 2016. http://dx.doi.org/10.1016/J.ADDR.2016.06.012

[18] M. Ouhsti, B. El Haddadi, S. Belhouideg, "Effect of Printing Parameters on the Mechanical Properties of Parts Fabricated with Open-Source 3D Printers in PLA by Fused Deposition Modeling", *Mechanics and Mechanical Engineering*, Vol. 22, No. 4, pp. 895–907, 2018.

[19] J. M. Reverte, M. A. Caminero, J. M. Chacon, E. Garcia-Plaza, P. J. Nunez and J. P. Becar, "Mechanical and Geometric Performance of PLA-Based Polymer Composites Processed by the Fused Filament Fabrication Additive Manufacturing Technique", *Materials*, 13, 1924, 2020. DOI: 10.3390/ma13081924.

[20] A. E. Babenko, M. I. Bobyr, O. O. Boronko, S. I. Trubachev, "Theory of vibrations and stability of motion: a collection of tasks for course design and practical classes for students of the training direction 6.050501 "Applied Mechanics", *NTUU "KPI"*, 2010.

[21] A. E. Sheinblit, "Course design of machine parts", *Yantar*, 2002.

[22] L. Safai, J.S. Cuellar, G. Smit, A.A. Zadpoor, "A review of the fatigue behavior of 3D printed polymers", *Additive Manufacturing*, 28, pp. 87–97, 2019. https://doi.org/10.1016/j.addma.2019.03.023